
BENCHMARKING OF QUERY STRATEGIES: TOWARDS FUTURE DEEP ACTIVE LEARNING

BENCHMARK PAPER

Shiryu Ueno

Dept. of Natural Science and Technology
Gifu University
ueno@cv.info.gifu-u.ac.jp

Yusei Yamada

Dept. of Natural Science and Technology
Gifu University
yyamada@cv.info.gifu-u.ac.jp

Shunsuke Nakatsuka

Dept. of Natural Science and Technology
Gifu University, Panasonic
nakatsuka@cv.info.gifu-u.ac.jp

Kunihito Kato

Dept. of Natural Science and Technology
Gifu University
kato.kunihito.k6@f.gifu-u.ac.jp

December 12, 2023

ABSTRACT

In this study, we benchmark query strategies for deep active learning (DAL). DAL reduces annotation costs by annotating only high-quality samples selected by query strategies. Existing research has two main problems, that the experimental settings are not standardized, making the evaluation of existing methods is difficult, and that most of experiments were conducted on the CIFAR or MNIST datasets. Therefore, we develop standardized experimental settings for DAL and investigate the effectiveness of various query strategies using six datasets, including those that contain medical and visual inspection images. In addition, since most current DAL approaches are model-based, we perform verification experiments using fully-trained models for querying to investigate the effectiveness of these approaches for the six datasets. Our code is available at .

1 Introduction

Deep learning requires a large annotated dataset. The annotation cost in terms of time and money, is high when the target task requires professional experience, such as for medical and visual inspection images. Deep active learning (DAL) Ren et al. [2021], Zhan et al. [2022], Takezoe et al. [2022] is a method that maintains or improves model performance while limiting the annotation cost. DAL approaches can be divided into membership query synthesis Angluin [1988], stream-based sampling Malialis et al. [2020], and pool-based sampling McCallum and Nigam [1998]. In membership query synthesis, the model generates high-quality samples for learning. In stream-based sampling, the model judges whether new samples in a data stream should be labeled. In pool-based sampling, the model selects high-quality samples for annotation from a pool of unlabeled data. This study focuses on pool-based sampling, which is widely used in existing studies.

Figure 1 shows a typical DAL framework. As shown, DAL repeats the cycle of query, annotation, and training under the annotation budget or target accuracy. Querying refers to the selection of samples. By constructing training data with high-quality samples in each cycle, DAL can quickly reach the target accuracy, reducing the annotation cost.

In studies on DAL, the hyperparameters related to the number of training data (e.g., number of queried data $|\mathcal{Q}_c|$ or total number of cycles C) and other experimental settings (e.g., model initialization settings at the beginning of each cycle) are not standardized. In addition, the random seed is not fixed in some experiments, making a performance comparison of existing methods difficult. Many of the reported experiments were performed on the CIFAR Krizhevsky [2009] or MNIST Lecun et al. [1998] dataset, both of which are homogeneous (i.e., balanced and clean). However, DAL is expected to be used with more practical datasets (e.g., medical or visual inspection images), which are imbalanced or

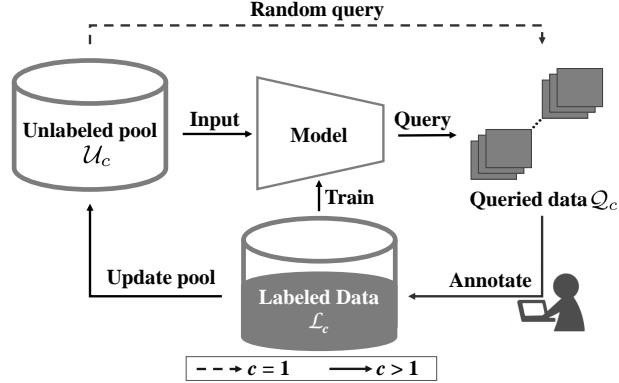


Figure 1: Framework of DAL. In cycle c , a model trained on labeled data \mathcal{L}_c selects useful queried data \mathcal{Q}_c from the unlabeled pool \mathcal{U}_c . In cycle $c+1$, the process is repeated with $\mathcal{L}_{c+1} = \mathcal{L}_c + \mathcal{Q}_c$ and $\mathcal{U}_{c+1} = \mathcal{U}_c - \mathcal{Q}_c$. In the first cycle ($c=0$), \mathcal{Q}_c is randomly selected.

noisy. Therefore, in this study, we develop a standardized experimental settings for DAL and investigate the effectiveness of various query strategies with six datasets, including those that contain medical or visual inspection images.

In addition, as shown in Figure 1, \mathcal{Q}_c is queried by models trained on labeled data \mathcal{L}_c . However, when $|\mathcal{L}_c|$ is small, the model may not be sufficiently trained and thus may not extract good features. In this case, query strategies based on features do not work well, and high-quality \mathcal{Q}_c cannot be obtained. To provide guidelines for future DAL studies, we perform verification experiments to compare the results of the currently used framework (Figure 1) with the results of a framework that uses a fully-trained model for queries. A fully-trained model can query \mathcal{Q}_c independent of the value of $|\mathcal{L}_c|$. Through the verification experiments, we investigate the effectiveness of the current DAL approach, which depends on the number of training data.

Our contributions are as follows.

- We show the inconsistency of experimental settings in reported experiments on DAL and the difficulty of comparing the performance of existing methods due to this inconsistency. To overcome this problem, we develop standardized experimental settings for DAL and use them to benchmark existing methods.
- In addition to homogeneous datasets, we benchmark existing methods with datasets of medical or visual inspection images. We also perform experiments using pre-training with self-supervised learning to investigate the effectiveness of self-supervised learning for DAL.
- We perform verification experiments with a fully-trained model for querying \mathcal{Q}_c and compare the results with those in the benchmarking experiments. We show that developing a query strategy based on the current DAL approach and verifying its effectiveness for a homogeneous dataset is difficult and that doing so far a non-homogeneous dataset would be beneficial. We also show the importance of considering the characteristics of the target dataset when developing a query strategy.

2 Related Work

2.1 Query Strategies

DAL aims to reduce annotation costs by querying only high-quality samples with query strategies. The query strategies can be categorized into uncertainty-based, representative/diversity-based, and hybrid strategies.

2.1.1 Uncertainty-based query strategies

Uncertainty-based query strategies select uncertain samples by using sample complexity or ambiguity. This is based on the concept that uncertain samples contain useful information for the model and should be labeled. Typical methods use the predicted probability of the model Lewis and Catlett [1994], Aljundi et al. [2022], the predicted probability distribution of Bayesian neural network Goan and Fookes [2020], Zhang et al. [2022], Gal et al. [2017], or the consistency of the model prediction Yu et al. [2022], Guo et al. [2022]. One major problem with uncertainty-based query strategies is that they tend to query samples near the boundary, and thus they select similar samples.

2.1.2 Representative/diversity-based query strategies

Representative/diversity-based query strategies select samples to broaden the distribution of the query data. This avoids the selection of similar samples, which is a problem with uncertainty-based query strategies. Typical methods use clustering Nguyen and Smeulders [2004], Geifman and El-Yaniv [2017], adversarial sampling Ducoffe and Precioso [2018], Zhu and Bento [2017], or generative models Sinha et al. [2019]. One major problem with representative/diversity-based methods is that they do not consider the uncertainty of data, so the model sometimes queries easy samples. In addition, methods that use clustering or adversarial sampling are computationally expensive compared with uncertainty-based methods.

2.1.3 Hybrid-based query strategies

Hybrid-based query strategies combine uncertainty-based methods and representative/diversity-based methods Shui et al. [2020], Yin et al. [2017]. This approach cancels out the disadvantages of each type of method. Some hybrid-based methods combine existing uncertainty-based methods and representative/diversity-based methods Zhdanov [2019]. As with representative/diversity-based methods, these methods often require clustering or adversarial sampling and are computationally expensive.

2.1.4 Issues with existing work

In previous studies, hyperparameters related to the number of training data and other experimental settings are not standardized. This leads to different performance even if $|\mathcal{L}_c|$ is the same Chen et al. [2022], Houlsby et al. [2014], Zhu et al. [2018]. In addition, the random seed was not fixed in some experiments, and thus comparing the performance of existing methods is difficult. To overcome these problems, we develop standardized experimental settings for DAL and use them to benchmark existing methods.

2.2 DAL for Medical or Visual Inspection Images

Most previous studies proposed query strategies and verified them using the CIFAR or MNIST dataset. Query strategies for medical or visual inspection images have also been proposed Logan et al. [2022a], Mehta et al. [2022]. For example, Logan et al. [2022b] proposed a method for querying a certain number of samples for each patient from their optical coherence tomography (OCT) Gholami et al. [2019] and X-Ray Kermany et al. [2018]. Pimentel et al. Pimentel et al. [2020] proposed unsupervised to active inference (UAI), which defines an anomaly metric for each sample using embedding expressions and anomaly scores with a denoising auto encoder Vincent et al. [2008]. They proposed a method for querying samples based on UAI.

The motivation for these studies was the assumption that existing methods proposed for the CIFAR and other homogeneous datasets do not work for medical or visual inspection images. However, to the best of our knowledge, this assumption has not been verified. Therefore, in this paper, we investigate the effectiveness of query strategies for medical or visual inspection images.

2.3 DAL for Imbalanced, Out-of-Distribution, or Noisy Data

When considering the practical use of DAL, the target datasets may include imbalanced Lemaître et al. [2017], out-of-distribution(OoD) Ovadia et al. [2019], or noisy labels Natarajan et al. [2013]. Therefore, some methods for datasets containing such labels have been proposed Bengar et al. [2021], Benkert et al. [2022], Li et al. [2022]. For example, Killamsetty et al. Killamsetty et al. [2021] proposed a method for querying a subset of data to maximize the log-likelihood for validation set using a submodular function Fujishige [2005] and showed its performance for imbalanced or noisy data. Kothawade et al. Kothawade et al. [2021] proposed the transformation of submodular mutual information (SMI) Gupta and Levin [2020], Iyer et al. [2021] into a form corresponding to imbalanced, OoD, or redundant data, and queried samples to maximize the SMI.

Because many previous studies verified their methods using artificial non-homogeneous datasets based on the CIFAR or MNIST dataset, which are homogeneous, it is unclear whether they work on datasets that contain actual non-homogeneous data, such as medical or visual inspection images. Furthermore, most existing methods require prior knowledge of the imbalanced or OoD characteristics in the datasets. However, in the DAL framework, the datasets are not initially annotated, making it impossible to know in advance their characteristics. Consequently, these methods are not practical in this context.

Table 1: Distribution of training and test data for EuroSAT dataset

Classes	training data	test data
Industrial Buildings	2,037	463
Residential Buildings	2,444	556
Annual Crop	2,445	555
Permanent Crop	2,037	463
River	2,037	463
Sea & Lake	2,444	556
Herbaceous Vegetation	2,445	555
Highway	2,037	463
Pasture	1,629	371
Foreset	2,445	555
Summary	22,000	2,200

2.4 DAL with Semi-Supervised Learning

Semi-supervised learning (semi-SL) Zhou and Zhou [2021], Van Engelen and Hoos [2020] uses both labeled and unlabeled data. This matches the DAL framework and thus methods that combine DAL and semi-SL have been proposed. For example, Gao et al. Gao et al. [2020] used the MixMatch Berthelot et al. [2019] framework of semi-SL to prepare a large amount of augmented data and query samples based on the consistency of model prediction. Yuan et al. Yuan et al. [2022], proposed a combination of the FixMatch Sohn et al. [2020] framework and contrastive learning Chen et al. [2020], He et al. [2020] to train models using both labeled and unlabeled data. Samples are queried using the trained models. MixMatch and FixMatch require strong data augmentation and are thus ineffective for non-natural images. Due to this limitation, we do not utilize a combination of semi-SL and DAL in this study.

2.5 DAL with Self-Supervised Learning

Self-supervised learning (self-SL) Jaiswal et al. [2020] uses unlabeled data with mechanically generated labels, called Pretext Task Trinh et al. [2019], Misra and van der Maaten [2020] or contrastive learning. Since self-SL does not require labeled data for learning, it is often used as a pre-training method. Furthermore, methods that combine self-SL with DAL have been proposed. For example, Yi et al. Yi et al. [2022], proposed a method that utilizes angle prediction as a pretext task for pre-training, and queries samples based on the loss of the pretext task. Caramalau et al. Caramalau et al. [2022], replaced the encoder of MoBY Xie et al. [2021], a self-SL method proposed for the Swin-Transformer Liu et al. [2021], with a CNN. They then modified the framework to enable MoBY to learn from not only unlabeled data but also labeled data. Samples are queried using the trained model.

However, these studies performed experiments using the CIFAR or MNIST dataset. In this paper, we investigate the effectiveness of self-SL with DAL not only for homogeneous datasets, but also for non-homogeneous datasets by performing experiments using pre-training with SimSiam Chen and He [2020].

3 Experiments: Benchmarking of Query Strategies

3.1 Datasets

In this paper, we use CIFAR10 for natural images, EuroSAT for satellite images Helber et al. [2017], OCT and BrainTumor for medical images Cheng, Jun [2017], GAPS and KolektorSDD2 for visual inspection images Stricker et al. [2019], Božič et al. [2021].

CIFAR10 is a natural image dataset with 50,000 training data and 10,000 test data, and consists of 10 classes with an equal number of data per class. The image size is 32×32 pixels. We use RandomCrop and RandomHorizontalFlip with a probability of $p = 0.5$ as data augmentation.

EuroSAT is a satellite image dataset consisting of 10 classes and a total of 27,000 data, with a relatively equal number of data per class. The image size is 64×64 pixels. In accordance with previous studies Cheng et al. [2020], Radford et al. [2021], we use 22,000 data for training and 5,000 data for testing. The distribution of the number of data per class after splitting EuroSAT is shown in Table 1. We use RandomVerticalFlip with a probability of $p = 0.5$ as data augmentation.

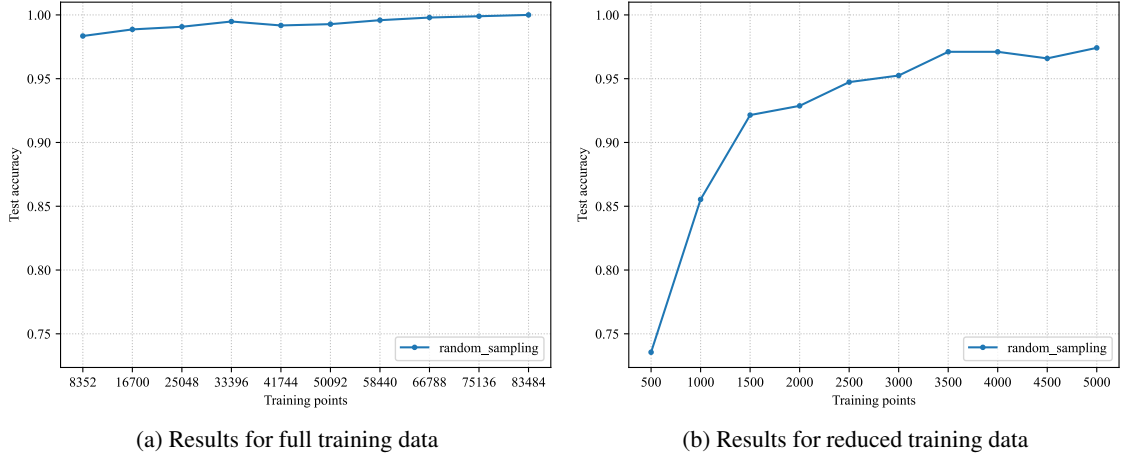


Figure 2: Results obtained with various numbers of training data for OCT

Table 2: Distribution of full and reduced training data for OCT dataset

Classes	full data	reduced data
NORMAL	26,315	1,576
CNV	37,205	2,229
DME	11,348	679
DRUSEN	8,616	516
Summary	83,484	5,000

Table 3: Distribution of training and test data for BrainTumor dataset

Classes	training data	test data
Glioma	1,139	287
Meningioma	542	166
Pituitary Tumor	740	190
Summary	2,421	643

OCT is a medical image dataset of gray-scale cross-sectional images of retinas with 83,484 training data and 968 test data, and consists of four classes. OCT is an imbalanced dataset. The image size is not uniform, so we resized the images to 224×224 pixels. Figure 2 (a) shows the results of DAL obtained using the full training data of OCT. As shown, when using the full training data, the accuracy in the first cycle is approximately 98%; it stays within 98-100% in subsequent cycles. Therefore, the difference in accuracy between the methods is at most about 1%. This difference can be considered to be error, making it difficult to compare the methods. To address this issue, we randomly reduced the training data from 83,484 to 5,000 data while maintaining the distribution of the classes. Figure 2 (b) shows the results of DAL obtained with the reduced dataset. As shown, the improvement in accuracy is significant. It is likely that the difference in accuracy between the methods is greater than the error. The distribution of the number of training data per class after the reduction of OCT is shown in Table 2.

BrainTumor is a medical image dataset of gray-scale magnetic resonance imaging images of the brain with a total of 3,064 data, and consists of three classes. BrainTumor is an imbalanced dataset. The image size is 512×512 pixels, which is rather large, so we resized the images to 256×256 pixels. BrainTumor is provided with five-fold cross-validation. Therefore, in this paper, we split the data into training and test data with a ratio of 4:1. The distribution of the number of training data per class after splitting BrainTumor is shown in Table 3.

GAPs is a dataset of visual inspection images of asphalt surfaces taken in Germany. There are three types of data: GAPs 10m, GAPs v2, and GAPs v1. In this paper, we use GAPs v2, which is available for image classification. GAPs consists of 2,468 gray-scale images with a size of 1920×1080 pixels. The images can be divided into patches of arbitrary sizes. In accordance with previous studies Stricker et al. [2019], the patch size was set to 64×64 pixels. GAPs includes 50,000 training data and 10,000 test data. It is strongly imbalanced. Moreover, GAPs includes noise-labeled data.

KolektorSDD2 is a dataset of gray-scale visual inspection images of the surfaces of manufactured products. It has 2,331 training data and 1,004 test data. KolektorSDD2 is strongly imbalanced. The image size is 230×630 pixels, so we resized the images to 224×224 pixels. KolektorSDD2 is a dataset for segmentation, so only the training data annotations for classification are provided. Therefore, we annotated the 110 NG (anomaly) samples in the test data based on Božič et al. [2021] and segmentation ground truth.

Using these datasets, we investigate the effectiveness of existing query strategies using medical and visual inspection images. Furthermore, since BrainTumor, OCT, GAPs, and KolektorSDD2 are imbalanced datasets, we investigate the effectiveness of these strategies on imbalanced data. Moreover, since GAPs contains noise-labeled data, we investigate the effectiveness of existing query strategies on a noisy dataset using results from GAPs.

3.2 Methods

In this paper, we use Random Sampling, Entropy Sampling, BatchBALD Kirsch et al. [2019], k-means Sampling, Core-set Sener and Savarese [2018], BADGE Ash et al. [2019], and Cluster Margin Citovsky et al. [2021].

Random Sampling randomly queries samples from the unlabeled pool \mathcal{U}_c . As other methods query samples strategically, Random Sampling is considered to be a baseline for evaluating the effectiveness of query strategies.

Entropy Sampling queries samples with large values for Equation (1).

$$H = p(\mathbf{y}|\mathbf{x})\log p(\mathbf{y}|\mathbf{x}) \quad (1)$$

where \mathbf{x} is an unlabeled data, \mathbf{y} is the class label, and $p(\mathbf{y}|\mathbf{x})$ is the model’s predicted probability.

BatchBALD queries samples that maximize the mutual information of the predicted probability distribution of a Bayesian neural network, as shown in Equation (2).

$$H(\mathbf{y}|\mathbf{x}, \mathcal{L}_{c-1}) - E_{p(\omega|\mathcal{L}_{c-1})}[H(\mathbf{y}|\mathbf{x}, \omega, \mathcal{L}_{c-1})] \quad (2)$$

where E is the expected value and ω is the model’s parameter distribution. In this study, we use monte-carlo (MC) dropout Gal and Ghahramani [2016] instead of a Bayesian neural network. While normal dropout is only performed during training, MC dropout is also performed during testing. By repeatedly performing testing with dropout and averaging the results, it is possible to approximate the distribution of each weight and estimate the distribution of the test results. The number of MC dropout iterations is a hyperparameter, but since it is impossible to perform hyperparameter optimization (i.e., parameter tuning) in DAL, we fix the number of MC dropout iterations to 40, following a previous study Beck et al. [2021].

k-means Sampling performs k-means clustering Macqueen [1967], with the number of clusters set to the number of query data $|\mathcal{Q}_c|$, and queries the sample closest to the centroid of each cluster.

Core-set uses the k-center problem Gert W Wolf [2011] to query the subset of \mathcal{U}_{c-1} . However, solving the k-center problem is NP-hard, so Core-set uses the k-center greedy approach to query samples that satisfy Equation (3).

$$\operatorname{argmax}_{i \in \mathcal{U}_{c-1}} \min_{j \in \mathcal{L}_{c-1}} d(f_i, f_j) \quad (3)$$

where d is a distance function and f represents features.

BADGE performs k-means++ Clustering Arthur and Vassilvitskii [2007] using the gradient vectors of unlabeled data. k-means++ Clustering alleviates the problem of initialization dependence in k-means Clustering by performing initialization using distances between data. By using gradient vectors, BADGE can consider sample uncertainty, and by using k-means++ Clustering, it can also consider sample diversity.

The framework of Cluster Margin is shown in Figure 3. First, hierarchical clustering is performed once. Then, during each query, Random Sampling is performed from small clusters in the order of small values for Equation 4.

$$\max_{i \in \mathcal{U}_{c-1}} (p(\mathbf{y}|\mathbf{x}_i)) - \max_{j \neq i, j \in \mathcal{U}_{c-1}} (p(\mathbf{y}|\mathbf{x}_j)) \quad (4)$$

By using hierarchical clustering, Cluster Margin can consider sample diversity, and by using Equation 4, it can also consider sample uncertainty. In addition, since hierarchical clustering is performed only once in Cluster Margin, the computational cost is relatively low.

We use the seven methods described above to investigate the effectiveness of uncertainty-based, representative/diversity-based, and hybrid query strategies for each dataset. In addition, there are query strategies that use a module to predict the loss Yoo and Kweon [2019] or a generative model Kim et al. [2021]. However, since these methods have different model structures than those of other query strategies, it is difficult to fairly evaluate their performance. Therefore, they are not used in this study.

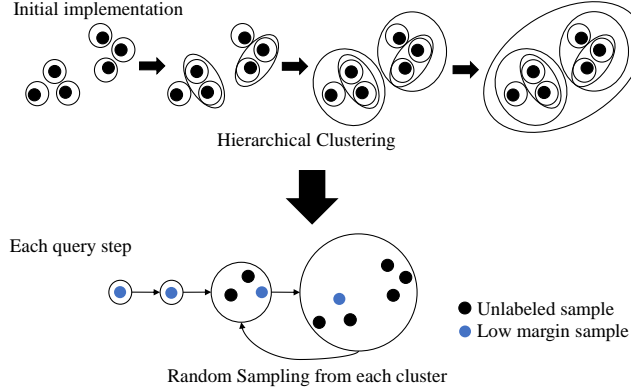


Figure 3: Framework of Cluster Margin

To investigate the effectiveness of self-SL for DAL, we conducted experiments using SimSiam for pre-training. SimSiam is a type of contrastive learning, where two different data augmentations are applied to each data, and learning is performed using twice as many augmented data. Augmented data from the same original data are positive pairs and those from different original data are negative pairs. Contrastive learning learns to increase the similarity between positive pairs and decrease the similarity between negative pairs. Many contrastive learning methods use a large batch size for similarity calculation with negative pairs. However, SimSiam learns only from positive pairs, making stable learning possible even with a small batch size.

3.3 Experimental Settings

3.3.1 Settings for DAL

For each dataset, $|\mathcal{Q}_c|$ is 10% of the entire training data and C is 10. For example, for CIFAR10, the model randomly queries 5,000 images in the first cycle, then strategically queries another 5,000 images and learns with a total of 10,000 labeled data in the next cycle. However, since BrainTumor and KolektorSDD2 have fractions in their training data, we randomly query the fractions in the first cycle. At the beginning of each cycle, we initialize the model weights. When we use pre-training, we initialize the model weights with pre-trained weights. We refer to these settings as scratch and self-SL, respectively. For each dataset, we evaluate the results using the average for five seeds. The evaluation metric is accuracy for the test data, except for GAPS and KolektorSDD2, where accuracy evaluation is difficult due to a strong imbalance in visual inspection images. Therefore, for these two datasets, we use F1-score Sokolova et al. [2006] for the test data. GAPS training is a six-class classification (one normal class and five anomaly classes). For testing, we treat the five anomaly classes as one class, resulting in a two-class classification.

3.3.2 Settings for deep learning

For all datasets, we use ResNet18 He et al. [2015] as the base model. For CIFAR10, for which the image size is very small (32×32 pixels), we modify the size of the convolutional kernel in the first layer from 7×7 to 3×3 . We set the batch size to 20, use the stochastic gradient descent optimizer with a learning rate of 0.01, a momentum of 0.9, and a weight decay of 0.0005, and train the model for 200 epochs. We also apply cosine decay to the learning rate.

3.3.3 Settings for SimSiam

For SimSiam, we use the output of ResNet18 up to just before the final classification layer as the encoder. For CIFAR10, we modify the convolutional kernel in the first layer from 7×7 to 3×3 . We set the batch size to 128, use the stochastic gradient descent optimizer with a learning rate of 0.05, a momentum of 0.9, and a weight decay of 0.0005, and train the model for 800 epochs. We also apply cosine decay to the learning rate. The data augmentations used for SimSiam are ResizedCrop, ColorJitter, Grayscale, GaussianBlur, and HorizontalFlip, similar to BYOLGrill et al. [2020]. The probabilities are $q = 0.8$ for ColorJitter, $q = 0.2$ for Grayscale, and $q = 0.5$ for the other augmentations. We do not use Grayscale for OCT, BrainTumor, GAPS, and KolektorSDD2, for which the original images are gray-scale.

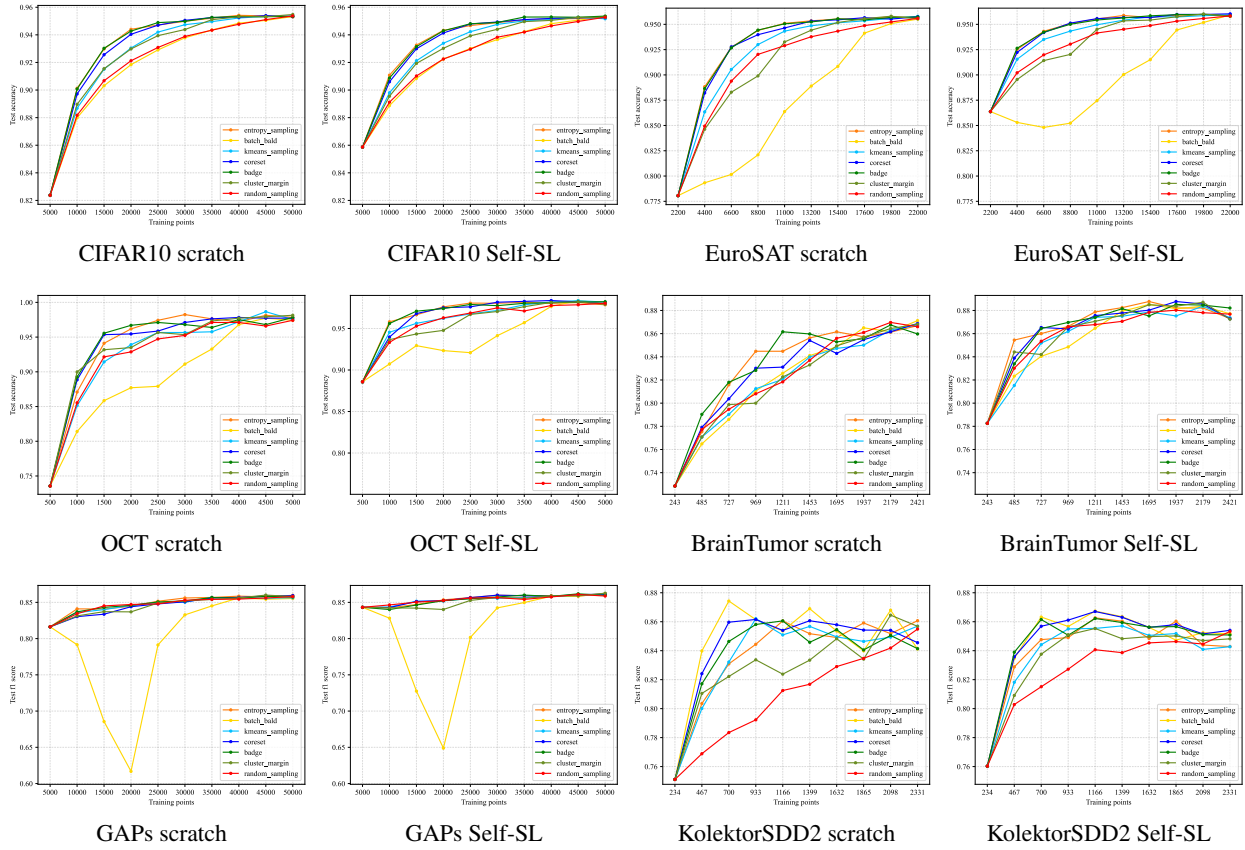


Figure 4: Result of benchmark. The horizontal axis represents the number of annotated samples and the vertical axis represents the corresponding test accuracy(or F1-score). By using query strategies, the model can reach the final accuracy of Random Sampling earlier, indicating that annotation cost can be reduced.

3.4 Benchmark Results

The results of the experiments are shown in Figure 4. The horizontal axis represents the number of annotated samples and the vertical axis represents the corresponding test accuracy (or F1-score) . By using query strategies, the model can reach the final accuracy of Random Sampling earlier, indicating that annotation cost can be reduced.

For CIFAR10, Entropy Sampling, Core-set, and BADGE reach the same accuracy at 35,000 data as that obtained training on all data, resulting in a 30% reduction in annotation cost. K-means Sampling and Cluster Margin reach the same accuracy at 40,000 data as that obtained training on all data, resulting in a 20% reduction in annotation cost. In contrast, BatchBALD performs similarly to Random Sampling and thus does not reduce the annotation cost. These results indicate that for CIFAR10, Entropy Sampling, Core-set, and BADGE are the most effective methods, followed by K-means Sampling and Cluster Margin, while BatchBALD performs poorly. The same results were observed for EuroSAT.

For OCT and BrainTumor, Entropy Sampling, Core-set, and BADGE showed high performance. The other query strategies had the same performance as that of Random Sampling. This suggests that some query strategies are effective even for medical images.

For GAPS, the score did not improve even as the number of labeled data $|\mathcal{L}_c|$ increased. This is because GAPS contains noisy data, and DAL cannot consider noisy labels during the query phase because annotation is performed after querying. Therefore, robust learning methods such as datacleansing Ridzuan and Wan Zainon [2019], Song et al. [2022] or framework improvements are required.

For KolektorSDD2, BatchBALD obtained the highest score at 700 labeled samples. To investigate the reason for this, we show the distribution of labeled data (from 234 to 700 samples) for the high-performing BatchBALD and the low-performing Entropy Sampling in Figure 5. As shown, BatchBALD queries NG samples early on, which mitigates

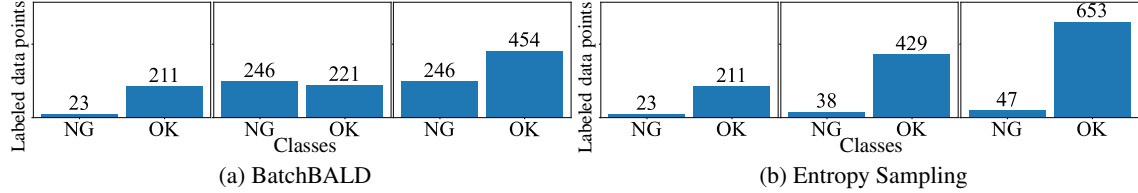


Figure 5: Distribution of training data in the first three cycles of KolektorSDD2. With BatchBALD, a large number of NG samples were queried early on, resulting in balanced learning and a significant improvement in performance in the early stages. In contrast, with Entropy Sampling, a large number of OK samples were queried, resulting in more imbalanced learning and a decrease in performance.

Table 4: Performance of fully-trained model for various datasets

Dataset	Evaluation metric	Performance
CIFAR10	Test accuracy	95.48%
EuroSAT	Test accuracy	95.18%
OCT	Test accuracy	98.24%
BrainTumor	Test accuracy	89.26%
GAPs	Test f1 score	85.33%
KolektorSDD2	Test f1 score	89.80%

the data imbalance, whereas Entropy Sampling queries a large number of OK samples, resulting in an imbalance that is not alleviated and an initial lack of accuracy improvement in the cycle. However, since BatchBALD performs poorly on other datasets, it can only be used in limited problem settings, such as imbalanced binary classification (e.g., KolektorSDD2).

Except for visual inspection images, self-SL was found to be effective in reducing annotation cost compared to scratch, indicating the effectiveness of self-SL in DAL. Self-SL did not work well for visual inspection images, likely due to the small variation in the anomaly-free data of inspection images, which resulted in pre-training failure. For SimSiam, different data augmentations are applied to each sample to acquire two augmented data and learning is performed to increase their similarity. However, since anomaly-free data are similar to each other, the augmented data obtained from these data are also similar, and it may thus not be possible to sufficiently learn representations. Therefore, further performance improvement for visual inspection images is expected if pre-training using approaches other than contrastive learning is applied.

For CIFAR10 and EuroSAT, the performance of Entropy Sampling, Core-set, and BADGE are very close. This suggests that there is no difference in performance between these query strategies for these datasets, indicating the limits of existing DAL methods. The development of methods and the verification of their effectiveness for these datasets are thus difficult. In the next section, we conduct verification experiments.

4 Verification Experiments: Querying Using Fully-trained Model

In this section, we conduct verification experiments to investigate the effectiveness of the current DAL approach for various datasets. The performance limit of DAL is obtained by learning with the optimal labeled data \mathcal{L}_c^* in each cycle. However, obtaining the optimal \mathcal{L}_c^* requires solving a combinatorial problem, which is impractical. Therefore, we focus on the model-dependent approach of querying based on the model’s prediction probabilities or features in the current DAL method and modify the framework.

4.1 Framework and Settings for Verification Experiments

The framework used for the verification experiments is shown in Figure 6. In conventional DAL, querying is done by a model trained on \mathcal{L}_c . However, when $|\mathcal{L}_c|$ is small, the model’s learning can be insufficient, resulting in poor feature representations. Query strategies using such feature representations may not work sufficiently, and it may not be possible to query high-quality \mathcal{Q}_c . Therefore, we replace the model used for querying with a fully-trained model (i.e., a model trained on the entire training data) to query \mathcal{Q}_c that is independent of $|\mathcal{L}_c|$. We investigate whether current model-dependent DAL methods improve their performance by comparing the results of the verification experiments with the benchmark results presented in Section 3.4 and Figure 6.

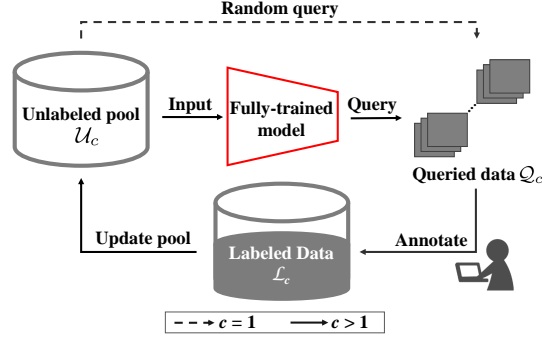


Figure 6: Framework for verification experiments

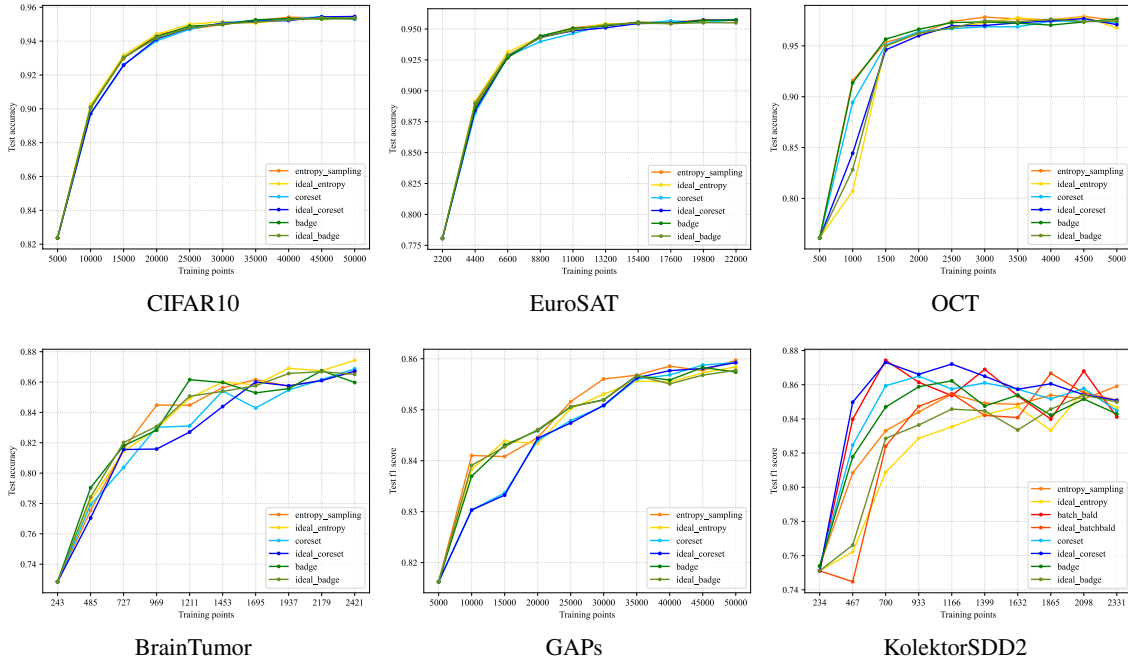


Figure 7: Results of verification experiments. Results of ideal_entropy, ideal_coreset, ideal_badge, and ideal_batchbald under the framework shown in Figure 6.

In the verification experiments, we use the same datasets as those in the benchmark and employ the query strategies that performed well: Entropy Sampling, Core-set, and BADGE. In addition, we use BatchBALD for KolektorSDD2 because it showed the best performance. We use the same hyperparameters as those in the benchmark and only perform learning from scratch. The performance of the fully-trained models used in each dataset is shown in Table 4.

4.2 Results of Verification Experiments

The results of the verification experiments are shown in Figure 7. As shown, there is no performance difference between the regular framework and the framework shown in Figure 6 for CIFAR10 and EuroSAT. However, performance differences were observed for other datasets, such as KolektorSDD2.

DAL achieves high performance with limited $|\mathcal{L}_c|$ by constructing \mathcal{L}_c with only high-quality data. Therefore, no performance difference was observed for homogeneous datasets such as CIFAR. On the other hand, for non-homogeneous datasets such as KolektorSDD2, performance differences were observed.

Thus, further development of DAL is expected if query strategies for datasets such as KolektorSDD2 are proposed. For designing such query strategies, it is necessary to consider the characteristics and purpose of the given dataset.

5 Conclusions

In this paper, we showed the problems of existing studies on DAL, such as non-standardized hyperparameters and limited datasets, and demonstrated that due to these problems, it is difficult to compare query strategies and evaluate the performance of DAL on medical or visual inspection images. We then developed standardized experimental settings as a baseline for future DAL research and investigated the effectiveness of various query strategies.

In benchmark experiments conducted to examine the effectiveness of existing query strategies, we confirmed their effectiveness not only on natural images but also on satellite, medical, and visual inspection images. Poor performance was observed for datasets that include noisy labels, such as GAPS, for which we confirmed that DAL itself does not function properly. Since annotation errors may occur in practical use, it is necessary to propose robust frameworks or learning methods for noisy labels. Furthermore, for all datasets except for visual inspection images, we confirmed that the use of self-SL in pre-training improves accuracy and increases the annotation cost reduction that can be achieved by DAL. However, we could not confirm the effectiveness of Self-SL on visual inspection images. This is thought to be due to the high similarity between anomaly-free data in visual inspection images. Therefore, applying effective self-SL methods to visual inspection images is expected to further reduce annotation costs.

Next, to investigate the effectiveness of the current DAL, we conducted verification experiments that compared the results obtained using a framework that uses a fully-trained model at each cycle during query and those obtained using a normal framework for existing datasets to verify for which datasets DAL is effective. The results of the verification experiments confirm that there is no performance difference for homogeneous datasets such as CIFAR10 and EuroSAT among the query strategies. In contrast, there was a performance difference for non-homogeneous datasets such as KolektorSDD2. This indicates that many current DAL methods do not show a significant improvement in performance for homogeneous datasets. These methods are not expected to improve significantly in the future. However, there is great potential for new query strategies for non-homogeneous datasets, which are encountered in practical use. Therefore, in the future, we need to develop query strategies that consider the characteristics and purpose of the given dataset to increase the effectiveness of DAL in practical applications.

References

- Pengzhen Ren, Yun Xiao, Xiaojun Chang, Po-Yao Huang, Zhihui Li, Brij B. Gupta, Xiaojiang Chen, and Xin Wang. A Survey of Deep Active Learning. In *ACM Computing Surveys*, pages 1–40, 2021.
- Xueying Zhan, Qingzhong Wang, Kuan-hao Huang, Haoyi Xiong, Dejing Dou, and Antoni B. Chan. A Comparative Survey of Deep Active Learning, 2022.
- Rinyoichi Takezoe, Xu Liu, Shunan Mao, Marco Tianyu Chen, Zhanpeng Feng, Shiliang Zhang, and Xiaoyu Wang. Deep Active Learning for Computer Vision: Past and Future, 2022.
- Dana Angluin. Queries and Concept Learning. *Machine Learning*, 2(4):319–342, 1988. ISSN 1573-0565.
- Kleanthis Malialis, Christos G. Panayiotou, and Marios M. Polycarpou. Data-efficient online classification with siamese networks and active learning. In *International Joint Conference on Neural Networks*, pages 1–7, 2020. ISBN 1-72816-926-7.
- Andrew McCallum and Kamal Nigam. Employing EM and Pool-Based Active Learning for Text Classification. In *International Conference on Machine Learning*, volume 98, pages 350–358, 1998.
- Alex Krizhevsky. Learning Multiple Layers of Features from Tiny Images. 2009.
- Yann Lecun, Léon Bottou, Yoshua Bengio, and Patric Haffner. Gradient-based learning applied to document recognition. *IEEE*, 86(11):2278–2324, 1998. ISSN 1558-2256.
- David D. Lewis and Jason Catlett. Heterogeneous Uncertainty Sampling for Supervised Learning. In *Machine Learning Proceedings 1994*, pages 148–156. 1994. ISBN 978-1-55860-335-6.
- Rahaf Aljundi, Nikolay Chumerin, and Daniel Olmeda Reino. Identifying Wrongly Predicted Samples: A Method for Active Learning. In *IEEE/CVF Winter Conference on Applications of Computer Vision*, pages 2071–2079, 2022. ISBN 978-1-66540-915-5.
- Ethan Goan and Clinton Fookes. Bayesian neural networks: An introduction and survey. *Cham: Springer International Publishing*, pages 45–87, 2020.
- Renyu Zhang, Aly A. Khan, Robert L. Grossman, and Yuxin Chen. BALanCe: Deep Bayesian Active Learning via Equivalence Class Annealing, 2022.
- Yarin Gal, Riashat Islam, and Zoubin Ghahramani. Deep Bayesian Active Learning with Image Data. In *International Conference on Machine Learning*, pages 1183–1192, 2017.

- Weiping Yu, Sijie Zhu, Taojiannan Yang, and Chen Chen. Consistency-based Active Learning for Object Detection. In *IEEE/CVF Conference on Computer Vision and Pattern Recognition*, pages 3951–3960, 2022.
- Jiannan Guo, Yangyang Kang, Yu Duan, Xiaozhong Liu, Siliang Tang, Wenqiao Zhang, Kun Kuang, Changlong Sun, and Fei Wu. Collaborative Intelligence Orchestration: Inconsistency-Based Fusion of Semi-Supervised Learning and Active Learning. In *ACM SIGKDD Conference on Knowledge Discovery and Data Mining*, pages 2935–2945, 2022.
- Hieu T. Nguyen and Arnold Smeulders. Active learning using pre-clustering. In *International Conference on Machine Learning*, page 79, 2004.
- Yonatan Geifman and Ran El-Yaniv. Deep Active Learning over the Long Tail, 2017.
- Melanie Ducoffe and Frederic Precioso. Adversarial Active Learning for Deep Networks: A Margin Based Approach, 2018.
- Jia-Jie Zhu and José Bento. Generative Adversarial Active Learning, 2017.
- Samarth Sinha, Sayna Ebrahimi, and Trevor Darrell. Variational Adversarial Active Learning. In *IEEE/CVF International Conference on Computer Vision*, pages 5972–5981, 2019.
- Changjian Shui, Fan Zhou, Christian Gagné, and Boyu Wang. Deep Active Learning: Unified and Principled Method for Query and Training. In *International Conference on Artificial Intelligence and Statistics*, pages 1308–1318, 2020.
- Changchang Yin, Buyue Qian, Shilei Cao, Xiaoyu Li, Jishang Wei, Qinghua Zheng, and Ian Davidson. Deep Similarity-Based Batch Mode Active Learning with Exploration-Exploitation. In *IEEE International Conference on Data Mining*, pages 575–584, 2017.
- Fedor Zhdanov. Diverse mini-batch Active Learning, 2019.
- Liangyu Chen, Yutong Bai, Siyu Huang, Yongyi Lu, Bihan Wen, Alan L. Yuille, and Zongwei Zhou. Making Your First Choice: To Address Cold Start Problem in Vision Active Learning, 2022.
- Neil Houlsby, Jose Miguel Hernandez-Lobato, and Zoubin Ghahramani. Cold-start Active Learning with Robust Ordinal Matrix Factorization. In *International Conference on Machine Learning*, pages 766–774, 2014.
- Yu Zhu, Jinhao Lin, Shibi He, Beidou Wang, Ziyu Guan, Haifeng Liu, and Deng Cai. Addressing the Item Cold-start Problem by Attribute-driven Active Learning. *IEEE Transactions on Knowledge & Data Engineering*, 32(04): 631–644, 2018.
- Yash-ye Logan, Ryan Benkert, Ahmad Mustafa, and Ghassan AlRegib. Patient aware active learning for fine-grained oct classification. In *International Conference on Image Processing*, pages 3908–3912, 2022a. ISBN 1-66549-620-7.
- Raghav Mehta, Changjian Shui, Brennan Nichyporuk, and Tal Arbel. Information Gain Sampling for Active Learning in Medical Image Classification. In *Uncertainty for Safe Utilization of Machine Learning in Medical Imaging: 4th International Workshop, UNSURE 2022, Held in Conjunction with MICCAI 2022, Singapore, September 18, 2022, Proceedings*, pages 135–145, 2022.
- Yash-ye Logan, Mohit Prabhushankar, and Ghassan AlRegib. DECAL: DEployable Clinical Active Learning, 2022b.
- Peyman Gholami, Priyanka Roy, Mohana Kuppaswamy Parthasarathy, and Vasudevan Lakshminarayanan. OCTID: Optical Coherence Tomography Image Database. *Computers & Electrical Engineering*, 81:106532, 2019.
- Daniel S. Kermany, Michael Goldbaum, Wenjia Cai, Carolina C. S. Valentim, Huiying Liang, Sally L. Baxter, Alex McKeown, Ge Yang, Xiaokang Wu, Fangbing Yan, Justin Dong, Made K. Prasadha, Jacqueline Pei, Magdalene Y. L. Ting, Jie Zhu, Christina Li, Sierra Hewett, Jason Dong, Ian Ziyar, Alexander Shi, Runze Zhang, Lianhong Zheng, Rui Hou, William Shi, Xin Fu, Yaou Duan, Viet A. N. Huu, Cindy Wen, Edward D. Zhang, Charlotte L. Zhang, Oulan Li, Xiaobo Wang, Michael A. Singer, Xiaodong Sun, Jie Xu, Ali Tafreshi, M. Anthony Lewis, Huimin Xia, and Kang Zhang. Identifying Medical Diagnoses and Treatable Diseases by Image-Based Deep Learning. *Cell*, 172(5):1122–1131.e9, 2018. ISSN 0092-8674, 1097-4172.
- Tiago Pimentel, Marianne Monteiro, Adriano Veloso, and Nivio Ziviani. Deep Active Learning for Anomaly Detection. In *International Joint Conference on Neural Networks*, pages 1–8, 2020.
- Pascal Vincent, Hugo Larochelle, Yoshua Bengio, and Pierre-Antoine Manzagol. Extracting and composing robust features with denoising autoencoders. In *International Conference on Machine Learning*, pages 1096–1103, 2008.
- Guillaume Lemaître, Fernando Nogueira, and Christos K. Aridas. Imbalanced-learn: A python toolbox to tackle the curse of imbalanced datasets in machine learning. *The Journal of Machine Learning Research*, 18(1):559–563, 2017.
- Yaniv Ovadia, Emily Fertig, Jie Ren, Zachary Nado, David Sculley, Sebastian Nowozin, Joshua Dillon, Balaji Lakshminarayanan, and Jasper Snoek. Can you trust your model’s uncertainty? evaluating predictive uncertainty under dataset shift. *Advances in neural information processing systems*, 32, 2019.

- Nagarajan Natarajan, Inderjit S. Dhillon, Pradeep K. Ravikumar, and Ambuj Tewari. Learning with noisy labels. *Advances in neural information processing systems*, 26, 2013.
- Javad Zolfaghari Bengar, Joost van de Weijer, Laura Lopez Fuentes, and Bogdan Raducanu. Class-Balanced Active Learning for Image Classification. In *IEEE/CVF Winter Conference on Applications of Computer Vision*, pages 1536–1545, 2021.
- Ryan Benkert, Mohit Prabhushankar, and Ghassan AlRegib. Forgetful Active Learning with Switch Events: Efficient Sampling for Out-of-Distribution Data. In *International Conference on Image Processing*, pages 2196–2200, 2022.
- Xingjian Li, Pengkun Yang, Tianyang Wang, Xueying Zhan, Min Xu, Dejing Dou, and Chengzhong Xu. Deep Active Learning with Noise Stability, 2022.
- Krishnateja Killamsetty, Durga Sivasubramanian, Ganesh Ramakrishnan, and Rishabh Iyer. GLISTER: Generalization based Data Subset Selection for Efficient and Robust Learning. In *AAAI Conference on Artificial Intelligence*, volume 35 of 9, pages 8110–8118, 2021.
- Satoru Fujishige. *Submodular Functions and Optimization*. Elsevier, 2005. ISBN 0-08-046162-X.
- Suraj Kothawade, Nathan Beck, Krishnateja Killamsetty, and Rishabh Iyer. Similar: Submodular information measures based active learning in realistic scenarios. *Advances in Neural Information Processing Systems*, 34:18685–18697, 2021.
- Anupam Gupta and Roie Levin. The online submodular cover problem. In *ACM-SIAM Symposium on Discrete Algorithms*, pages 1525–1537, 2020.
- Rishabh Iyer, Ninad Khargoankar, Jeff Bilmes, and Himanshu Asanani. Submodular combinatorial information measures with applications in machine learning. In *Algorithmic Learning Theory*, pages 722–754, 2021. ISBN 2640-3498.
- Zhi-Hua Zhou and Zhi-Hua Zhou. Semi-supervised learning. *Machine Learning*, pages 315–341, 2021.
- Jesper E. Van Engelen and Holger H. Hoos. A survey on semi-supervised learning. *Machine learning*, 109(2):373–440, 2020.
- Mingfei Gao, Zizhao Zhang, Guo Yu, Sercan O. Arik, Larry S. Davis, and Tomas Pfister. Consistency-based Semi-supervised Active Learning: Towards Minimizing Labeling Cost. In *Computer Vision—ECCV 2020*, pages 510–526, 2020.
- David Berthelot, Nicholas Carlini, Ian Goodfellow, Nicolas Papernot, Avital Oliver, and Colin A. Raffel. Mixmatch: A holistic approach to semi-supervised learning. *Neural Information Processing Systems*, 32, 2019.
- Xinkai Yuan, Zilinghan Li, and Gaoang Wang. Activematch: End-to-end semi-supervised active representation learning. In *2022 IEEE International Conference on Image Processing*, pages 1136–1140, 2022. ISBN 1-66549-620-7.
- Kihyuk Sohn, David Berthelot, Nicholas Carlini, Zizhao Zhang, Han Zhang, Colin A. Raffel, Ekin Dogus Cubuk, Alexey Kurakin, and Chun-Liang Li. Fixmatch: Simplifying semi-supervised learning with consistency and confidence. *Neural Information Processing Systems*, 33:596–608, 2020.
- Ting Chen, Simon Kornblith, Mohammad Norouzi, and Geoffrey Hinton. A simple framework for contrastive learning of visual representations. In *International Conference on Machine Learning*, pages 1597–1607, 2020. ISBN 2640-3498.
- Kaiming He, Haoqi Fan, Yuxin Wu, Saining Xie, and Ross Girshick. Momentum contrast for unsupervised visual representation learning. In *IEEE/CVF Conference on Computer Vision and Pattern Recognition*, pages 9729–9738, 2020.
- Ashish Jaiswal, Ashwin Ramesh Babu, Mohammad Zaki Zadeh, Debapriya Banerjee, and Fillia Makedon. A survey on contrastive self-supervised learning. *Technologies*, 9(1):2, 2020.
- Trieu H. Trinh, Minh-Thang Luong, and Quoc V. Le. Selfie: Self-supervised Pretraining for Image Embedding, 2019.
- Ishan Misra and Laurens van der Maaten. Self-supervised learning of pretext-invariant representations. In *IEEE/CVF Conference on Computer Vision and Pattern Recognition*, pages 6707–6717, 2020.
- John Seon Keun Yi, Minseok Seo, Jongchan Park, and Dong-Geol Choi. PT4AL: Using Self-Supervised Pretext Tasks for Active Learning, 2022.
- Razvan Caramalau, Binod Bhattarai, Danaïl Stoyanov, and Tae-Kyun Kim. MoBYv2AL: Self-supervised Active Learning for Image Classification. In *British Machine Vision Conference*, 2022.
- Zhenda Xie, Yutong Lin, Zhuliang Yao, Zheng Zhang, Qi Dai, Yue Cao, and Han Hu. Self-Supervised Learning with Swin Transformers, 2021.

- Ze Liu, Yutong Lin, Yue Cao, Han Hu, Yixuan Wei, Zheng Zhang, Stephen Lin, and Baining Guo. Swin transformer: Hierarchical vision transformer using shifted windows. In *IEEE/CVF International Conference on Computer Vision*, pages 10012–10022, 2021.
- Xinlei Chen and Kaiming He. Exploring Simple Siamese Representation Learning. In *IEEE/CVF Conference on Computer Vision and Pattern Recognition*, pages 15750–15758, 2020.
- Patrick Helber, Benjamin Bischke, Andreas Dengel, and Damian Borth. EuroSAT: A Novel Dataset and Deep Learning Benchmark for Land Use and Land Cover Classification. *IEEE Journal of Selected Topics in Applied Earth Observations and Remote Sensing*, 12(7):2217–2226, 2017.
- Cheng, Jun. Brain tumor dataset. figshare. Dataset. <https://doi.org/10.6084/m9.figshare.1512427.v5>, 2017.
- Ronny Stricker, Markus Eisenbach, Maximilian Sesselmann, Klaus Debes, and Horst-Michael Gross. Improving Visual Road Condition Assessment by Extensive Experiments on the Extended GAPs Dataset. In *International Joint Conference on Neural Networks*, pages 1–8, 2019.
- Jakob Božič, Domen Tabernik, and Danijel Skočaj. Mixed supervision for surface-defect detection: From weakly to fully supervised learning. *Computers in Industry*, 2021. ISSN 01663615.
- Gong Cheng, Xingxing Xie, Junwei Han, Lei Guo, and Gui-Song Xia. Remote Sensing Image Scene Classification Meets Deep Learning: Challenges, Methods, Benchmarks, and Opportunities. *IEEE Journal of Selected Topics in Applied Earth Observations and Remote Sensing*, 13:3735–3756, 2020. ISSN 2151-1535.
- Alec Radford, Jong Wook Kim, Chris Hallacy, Aditya Ramesh, Gabriel Goh, Sandhini Agarwal, Girish Sastry, Amanda Askell, Pamela Mishkin, and Jack Clark. Learning transferable visual models from natural language supervision. In *International Conference on Machine Learning*, pages 8748–8763, 2021. ISBN 2640-3498.
- Andreas Kirsch, Joost van Amersfoort, and Yarin Gal. BatchBALD: Efficient and Diverse Batch Acquisition for Deep Bayesian Active Learning. In *Neural Information Processing Systems*, volume 32, pages 7024–7035, 2019.
- Ozan Sener and Silvio Savarese. Active Learning for Convolutional Neural Networks: A Core-Set Approach. In *International Conference on Learning Representations*, 2018.
- Jordan T. Ash, Chicheng Zhang, Akshay Krishnamurthy, John Langford, and Alekh Agarwal. Deep Batch Active Learning by Diverse, Uncertain Gradient Lower Bounds, 2019.
- Gui Citovsky, Giulia DeSalvo, Claudio Gentile, Lazaros Karydas, Anand Rajagopalan, Afshin Rostamizadeh, and Sanjiv Kumar. Batch Active Learning at Scale. In *Neural Information Processing Systems*, volume 34, pages 11933–11944, 2021.
- Yarin Gal and Zoubin Ghahramani. Dropout as a Bayesian Approximation: Representing Model Uncertainty in Deep Learning. In *International Conference on Machine Learning*, pages 1050–1059, 2016.
- Nathan Beck, Durga Sivasubramanian, Apurva Dani, Ganesh Ramakrishnan, and Rishabh Iyer. Effective Evaluation of Deep Active Learning on Image Classification Tasks, 2021.
- J Macqueen. Some Methods for Classification and Analysis of Multivariate Observations. page 17, 1967.
- Gert W Wolf. Facility location: Concepts, models, algorithms and case studies. *Media*, 2011.
- David Arthur and Sergei Vassilvitskii. K-means++: The advantages of careful seeding. In *ACM-SIAM Symposium on Discrete Algorithms*, pages 1027–1035, 2007. ISBN 978-0-89871-624-5.
- Donggeun Yoo and In So Kweon. Learning Loss for Active Learning. In *IEEE/CVF Conference on Computer Vision and Pattern Recognition*, pages 93–102, 2019.
- Kwanyoung Kim, Dongwon Park, Kwang In Kim, and Se Young Chun. Task-aware variational adversarial active learning. In *IEEE/CVF Conference on Computer Vision and Pattern Recognition*, pages 8166–8175, 2021.
- Marina Sokolova, Nathalie Japkowicz, and Stan Szpakowicz. Beyond Accuracy, F-Score and ROC: A Family of Discriminant Measures for Performance Evaluation. In *AI 2006: Advances in Artificial Intelligence, Lecture Notes in Computer Science*, volume 4304, pages 1015–1021, 2006. ISBN 978-3-540-49787-5.
- Kaiming He, Xiangyu Zhang, Shaoqing Ren, and Jian Sun. Deep Residual Learning for Image Recognition. In *IEEE/CVF Conference on Computer Vision and Pattern Recognition*, pages 770–778, 2015.
- Jean-Bastien Grill, Florian Strub, Florent Alché, Corentin Tallec, Pierre Richemond, Elena Buchatskaya, Carl Doersch, Bernardo Avila Pires, Zhaohan Guo, and Mohammad Gheshlaghi Azar. Bootstrap your own latent—a new approach to self-supervised learning. In *Neural Information Processing Systems*, volume 33, pages 21271–21284, 2020.
- Fakhitah Ridzuan and Wan Mohd Nazmee Wan Zainon. A Review on Data Cleansing Methods for Big Data. *Procedia Computer Science*, 161:731–738, 2019. ISSN 1877-0509.
- Hwanjun Song, Minseok Kim, Dongmin Park, Yooju Shin, and Jae-Gil Lee. Learning from noisy labels with deep neural networks: A survey. *IEEE Transactions on Neural Networks and Learning Systems*, 2022.